

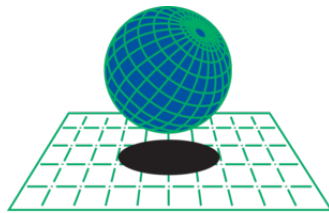
UNIVERSITAT POLYTECHNICA DE CATALUNYA
MSC COMPUTATIONAL MECHANICS
Spring 2018

Finite Element in Fluids

STOKES AND CAVITY FLOW

Due 01/06/2018

Alexander Keiser



CIMNE[®]



1 Stokes Problem

Here we will solve the Stokes problem with analytical solution and compute the pressure and velocity errors for various types of elements. We will first test the convergence for the Q_2Q_1 element. These plots of velocity error and pressure error can be seen below in figures 1 and 2 respectively.

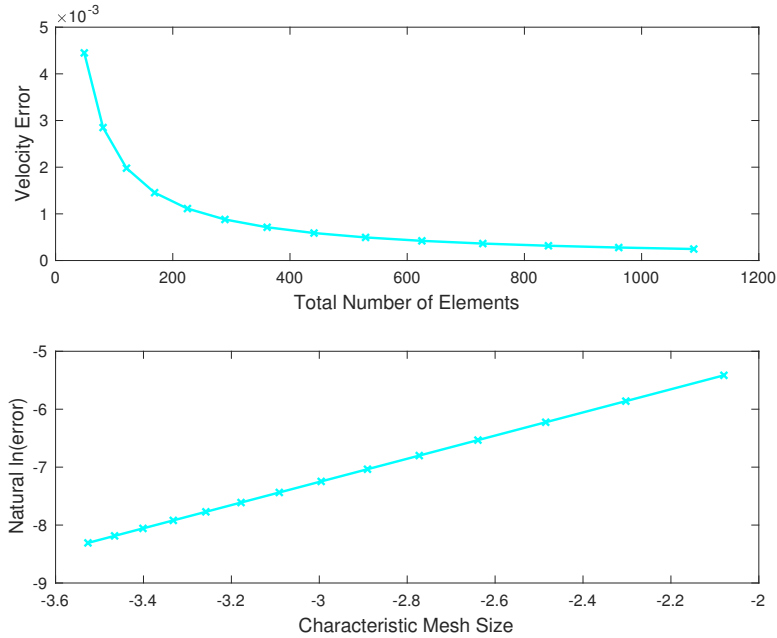


Figure 1: Q_2Q_1 Element Velocity Error

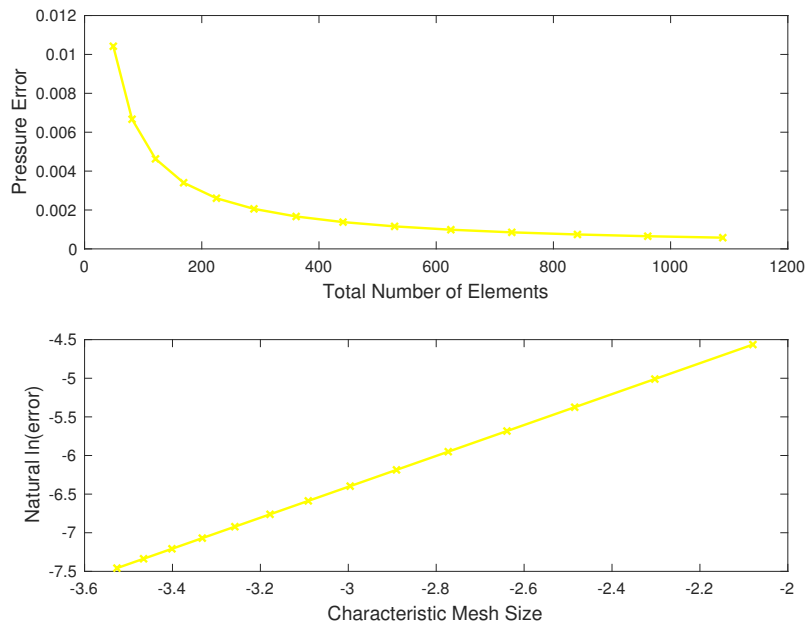


Figure 2: Q_2Q_1 Element Pressure Error

Above we can see the results for the convergence analysis of the Q_2Q_1 Element velocity and pressure errors. We can notice that we see good convergence in both the velocity and pressure errors. This is expected as the Q_2Q_1 element is robust and able to capture velocity and pressure behaviors accurately.

We will now examine the velocity and pressure error convergence for the Q_2Q_0 element. These results can be found below in figures 3 and 4 respectively.

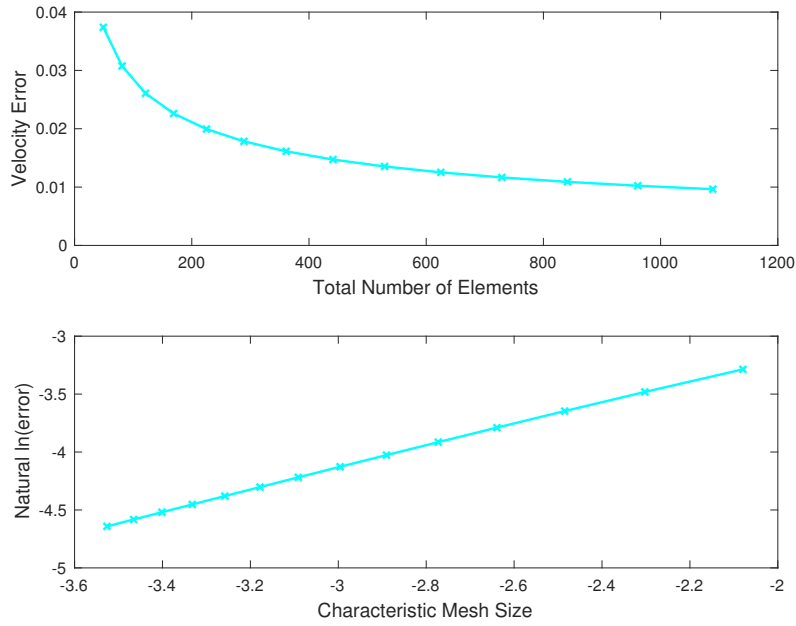


Figure 3: Q_2Q_0 Element Velocity Error

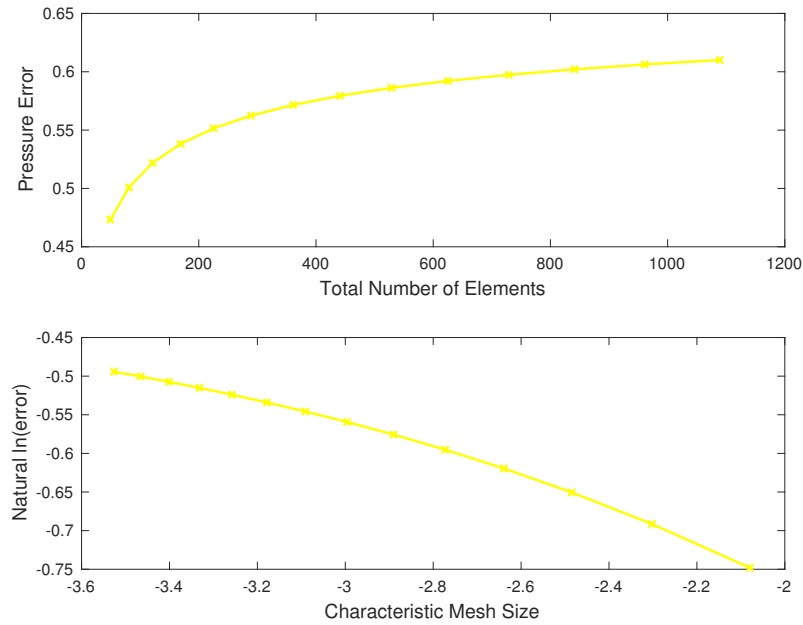


Figure 4: Q_2Q_0 Element Pressure Error

Above we can see the pressure and velocity convergence results for the Q_2Q_0 element. These results differ from the Q_2Q_1 . The velocity results exhibit good convergence, however the pressure error does not appear to converge to zero, but rather a value between 0.65 and 0.6. This could be explained by the Q_2Q_0 element's reduced ability to accurately capture pressure behavior.

We will now examine the velocity and pressure error convergence for the P_1P_1 element. These results can be found below in figures 5 and 6 respectively.

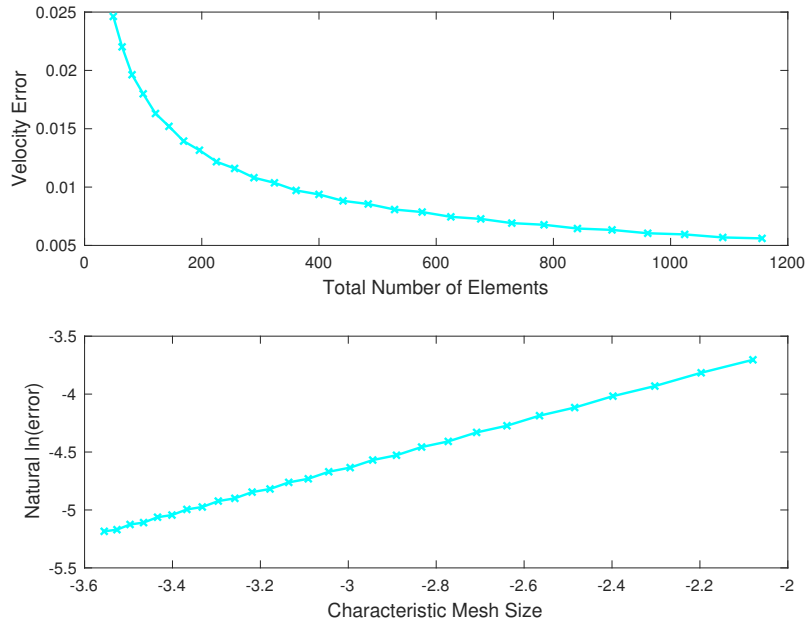


Figure 5: P_1P_1 Element Velocity Error

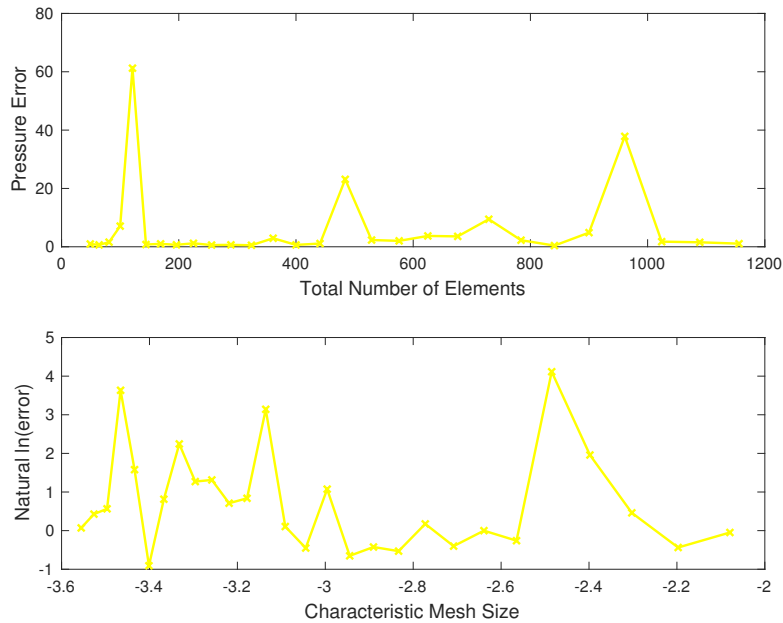


Figure 6: P_1P_1 Element Pressure Error

Above we can see the pressure and velocity convergence results for the P_1P_1 element. These results also differ from the previous results. The velocity results exhibit good convergence but have some very slight oscillatory behavior as seen in the top plot of figure 5. However, the pressure error exhibits much higher amounts of oscillatory behavior for some mesh sizes and number of elements. Others sizes exhibit much more accurate results. This can be explained by the use of P_1P_1 elements with an incorrectly stabilized formulation. These elements are much less robust at accurately capturing pressure and velocity behavior.

2 Cavity Flow Problem

We will analyze the solution to the cavity flow stokes problem utilizing a structured uniform and locally refined mesh of Q_2Q_1 Elements. The pressure and velocity field results for both of these mesh types can be seen below in figure 7 and 8.

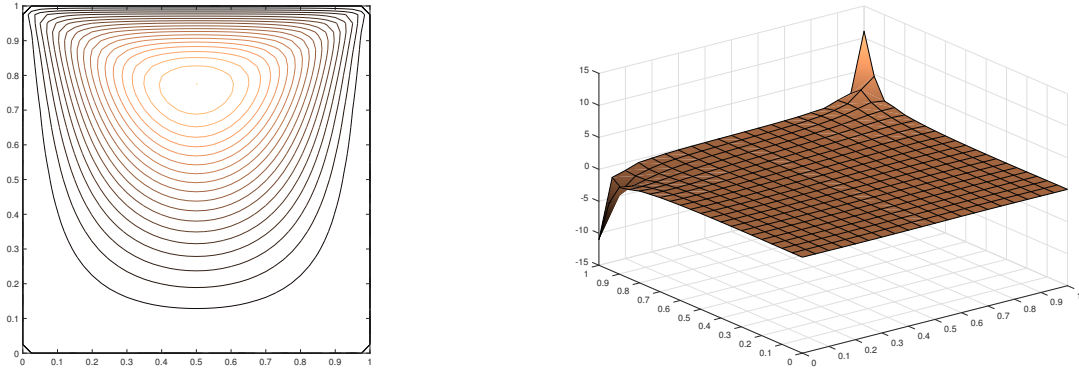


Figure 7: Velocity Field (left) and Pressure Field (right) results for Q_2Q_1 Elements Uniform Mesh

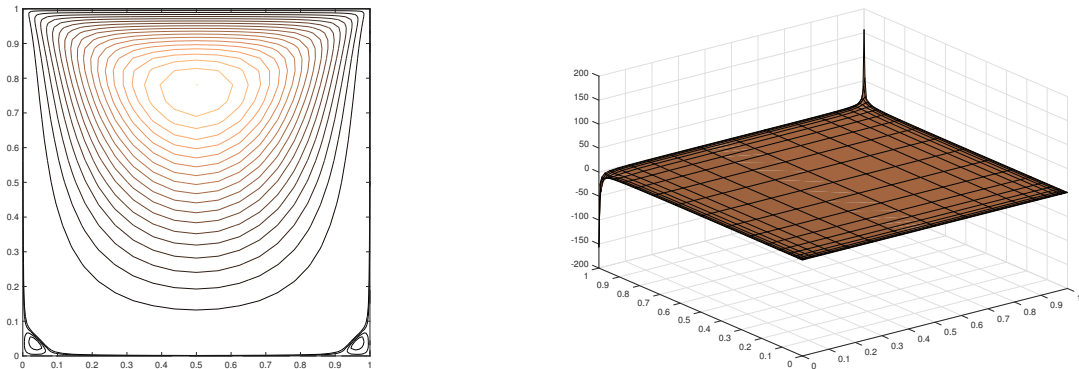


Figure 8: Velocity Field (left) and Pressure Field (right) results for Q_2Q_1 Elements Uniform Mesh

Above we can see the results for the uniform structured and locally refined Q_2Q_1 Element meshes. The first main difference between the two methods is the ability of the locally refined mesh to capture the small vortices behavior at the bottom left and bottom right of the velocity field in figure 8. The uniform mesh was not able to capture any of this behavior. Also, we can see that the pressure fields exhibit sharper and more accurate variations in the pressure profile. Due to these observations, it is fair to say that the local refined mesh near the walls produces more accurate results and is a better solution as it is better able to capture the specific behavior of that region. This is consistent with standard finite element methods of refining the mesh near areas of unique behaviors.

We will now solve the Navier-Stokes equations using the the Picard Method and a structured mesh of 20 Q_2Q_1 Elements per side. The results of this for various values of the Reynolds number can be seen on the next page in figures 9 through 12.

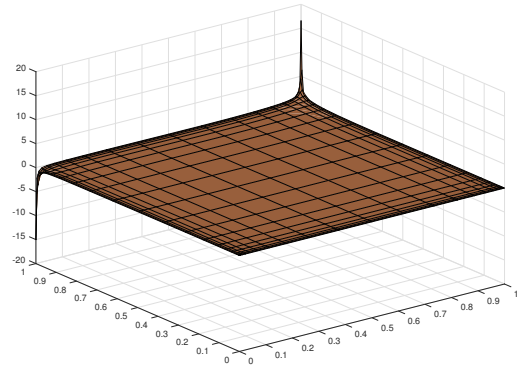
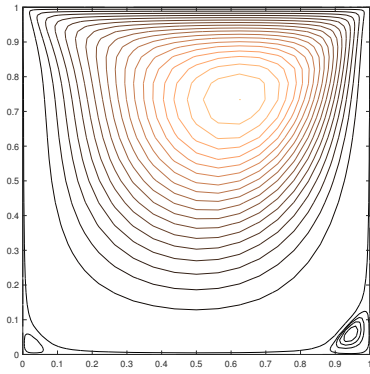


Figure 9: Velocity Field (left) and Pressure Field (right) results for Q_2Q_1 Re=100

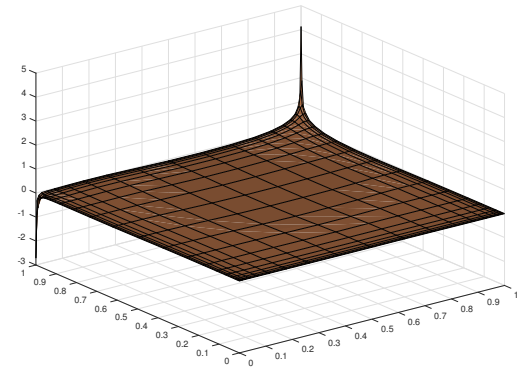
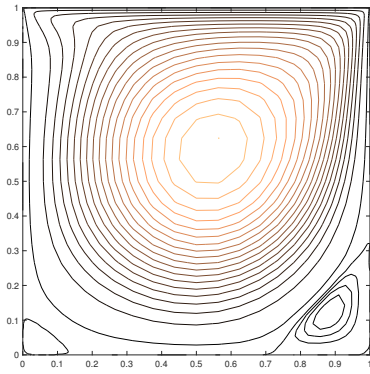


Figure 10: Velocity Field (left) and Pressure Field (right) results for Q_2Q_1 Re=500

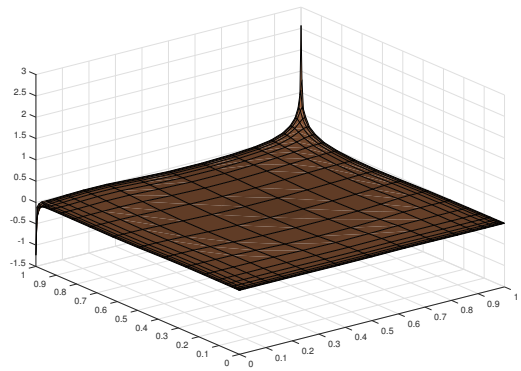
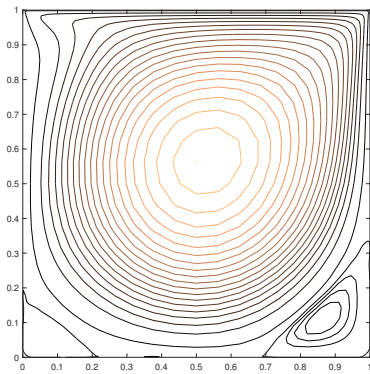


Figure 11: Velocity Field (left) and Pressure Field (right) results for Q_2Q_1 Re=1000

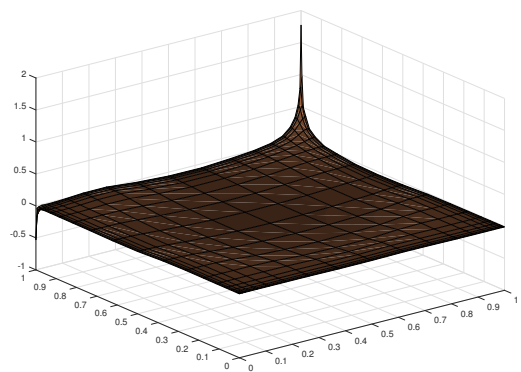
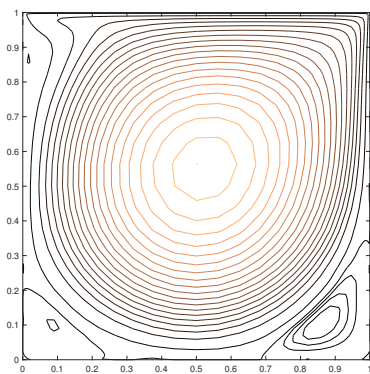


Figure 12: Velocity Field (left) and Pressure Field (right) results for Q_2Q_1 Re=2000

On the previous page we saw various pressure and velocity responses to different reynolds numbers when solving the classic cavity problem. We can notice that with each subsequent increase in reynolds number the magnitudinal variation of the pressure profile decreases. All four of these values are able to capture the bottom right vortex behavior. But we notice an increase in the size of the bottom right vortex at a reynolds number of 500. Additionally, at a reynolds number value of 2000, we can notice the development of an additional vortex in the bottom left hand corner.

We will now solve the same problem using an implemented Newton-Raphson method. The Newton-Raphson method has some advantages as it is a more robust method and converges more often than the picard method, which can fail under certain conditions. The Newton-Raphson method also is computationally more expensive per iteration but in theory should converge faster. Below in figure 13 we can see the results of a convergence analysis between the two methods and confirm the theory.

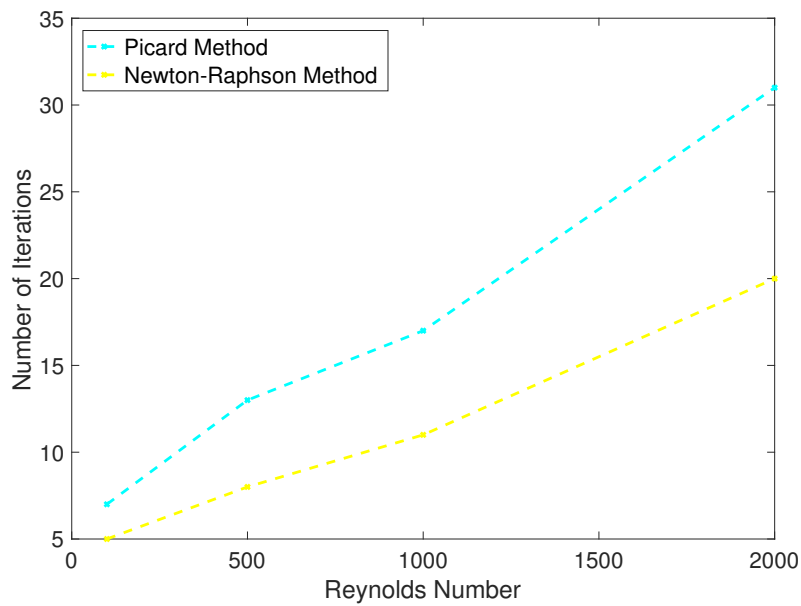


Figure 13: Iterations to Achieve Convergence